ELSEVIER

Journal of Nuclear Materials 241–243 (1997) 950–955

journal of nuclear materials

Plasma response on impurity injection in W7-AS

D. Hildebrandt [b,*], R. Brakel [a], A. Elsner [a], P. Grigull [a], H. Hacker [a], R. Burhenn [a], S. Fiedler [a], L. Giannone [a], C. Görner [a], H.J. Hartfuß [a], G. Herre [a], A. Herrmann [b], J.V. Hofmann [a], G. Kühner [a], D. Naujoks [b], F. Sardei [a], A. Weller [a], R. Wolf [b], W7-AS Team [a], ECRH Team [a], NBI Team [a]

[a] *EURATOM Association, Garching branch, Max-Planck-Institute of Plasma Physics, Garching, Germany*
[b] *EURATOM Association, Berlin branch, Max-Planck-Institute of Plasma Physics, Berlin, Germany*

Abstract

In order to study impurity transport and radiation behavior nitrogen has been injected into the scrape-off plasma of limiter-dominated discharges by gas puffing or into natural magnetic islands at the plasma edge of separatrix-dominated discharges by a reciprocating erosion probe. Strong radiative plasma edge cooling with a reduction of the power flux to the limiter could be obtained. The accompanied degradation of the energy confinement and the observed decrease of the central electron temperature can partly be explained by the reduction of the effective heating power. At high plasma densities and sufficiently strong impurity injection phenomena well known from tokamaks, like plasma shrinking, plasma detachment from the limiters and MARFE's were transiently observed.

Keywords: W7-AS; Stellarator; Boundary plasma; Radiation asymmetry; MARFE

1. Introduction

Significant power exhaust by radiation of impurities at the plasma edge is a promising possibility to reduce the power load to target plates in tokamaks or stellarators [1,2]. Configurational flexibility enables two approaches to radiative power exhaust to be examined in the W7-AS stellarator:

(1) A boundary photosphere of the core plasma may be established by injecting impurities from the edge into limiter bounded magnetic configurations.

(2) Impurities may specifically be injected and eventually confined into magnetic boundary islands in order to provide a local heat sink, topologically separated from the core plasma. For both scenarios experiments were initiated to explore impurity source and transport properties, the location of the impurity radiation, its impact on global confinement and on power balance, respectively.

2. Experiment

W7-AS has a fivefold toroidal magnetic symmetry which has recently been completed by installation of two graphite limiters in each of the five modules. They are located below and above the equatorial plane at the inboard side [3]. Depending on the rotational transform ι limiter-dominated operation with smooth flux surfaces (ι about $1/3$) or separatrix-dominated operation with natural magnetic islands at the plasma boundary (ι about $1/2$) can be realized. The limiters intersect these islands to a degree which can be controlled by ι and an additional vertical field.

In the first approach the radiation level is adjusted by nitrogen injection from a valve near the outboard wall. The gas flow can be adjusted either to a programmed flow rate, or feedback controlled to obtain a programmed radiation level. The intensity of the 76.5 nm line of N IV has been used as the control variable. The gas flow rate has been absolutely calibrated. Nitrogen was chosen as the injected gaseous impurity because it has favorable recycling and radiation behavior (see below). These experiments have

* Corresponding author. Tel.: +49-30 2036 6164; fax: +49-30 2036 6111; e-mail: hildebrandt@ipp-garching.mpg.de.

PII S0022-3115(96)00638-1

been performed in limiter-dominated discharges. W7-AS has been operated with a boronized wall.

In the second approach the impurities are to be injected into a region with magnetic islands which requires the impurity ion source to be localized with an accuracy of a few millimeters. This has been realized by impurity release from a reciprocating erosion probe. The probe has a stroke of 90 mm within 100 ms and stayed for a duration of about 20 ms at the reversal point in the plasma. It can be poloidally shifted from the bottom to the outboard side to reach O- or X-point regions. The cylindrical probe head consists of a boronnitrid-casing of about 5 mm diameter and length and a small electrode of titanium or carbon of 3 mm diameter and length on the front side. The probe was exposed to the plasma at floating potential or temporal biasing of the central electrode for measuring the incident particle flux and the electron temperature.

These experiments have been performed in NBI-heated discharges with a 5/9-island configuration which exhibits an island with a radial and poloidal extension of a few centimeters (see Fig. 1). The dominant injected impurity was nitrogen released from the BN-ceramics of the probe head.

In addition to standard diagnostics, the following diagnostics were available for measuring the plasma parameters and for investigating the transport and radiation behavior of the impurities. Different Langmuir probes (including the erosion probe), a high energy Li-beam, thermography of a lower limiter, two 30-channel bolometer systems (see Fig. 1), two 36 channel soft X-ray cameras without absorbing foils, a VUV-survey spectrometer (SPRED), a VUV-spectrometer equipped with a rotating mirror for poloidal scans, CCD-camera systems with Hα- and CIII-filters in video mode for observing a lower limiter surface and for

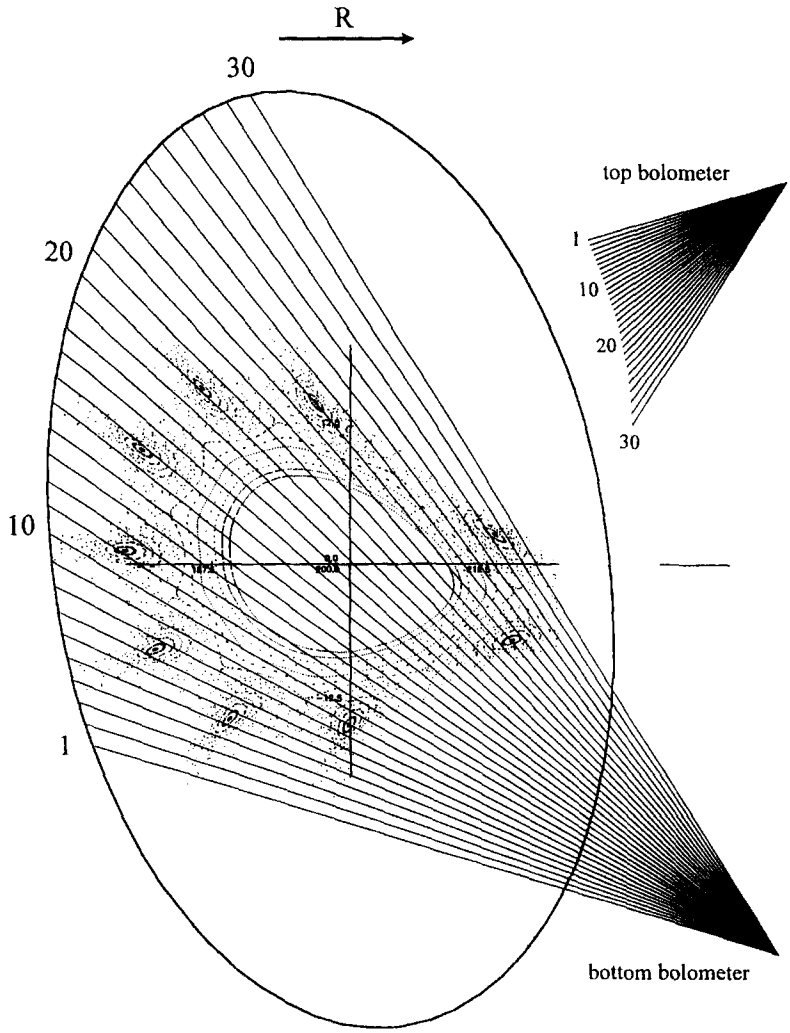

Fig. 1. Cross section of the magnetic configuration with magnetic islands at the boundary. Also shown are the chords of the bottom bolometer channels.

tangential plasma viewing. Total power losses by radiation and to the limiters are derived from the local bolometry and thermography measurements assuming toroidal symmetry.

3. Modelling of impurity transport and radiation

In order to describe the transport and radiation behavior of the injected impurities various models have been considered. In the case of limiter bounded plasmas with smooth flux surfaces the 1D radiation and transport code IONEQ [4] has been applied. 2D or. 3D modelling is necessary to describe the impurity behavior in a plasma edge with magnetic islands. These models using a Monte Carlo Code are presented in a separate paper [5]. Fig. 2 shows radiation profiles of the low Z impurities nitrogen and neon, and for comparison, of the medium Z impurity titanium calculated from the 1D-model for an ECRH-heated discharge (heating power 260 kW) with moderate density ($\langle n_e \rangle = 4 * 10^{19}$ m^{-3}).The following values were used: major radius $R = 2$ m, effective minor radius of the last closed flux surface (LCFS) $a = 0.18$ m, and of the wall $r_w = 0.20$ m, impurity diffusion coefficient 0.2 m^2/s, central electron temperature $T_e(0) = 1100$ eV, edge electron temperature $T_e(a) = 30$ eV. The total radiated power is kept fixed at the arbitrary value $P(r_w) = 100$ kW. For nitrogen and neon the gross radiation arises from Li- and Be-like ions. The maxima of the emissivity $Q(r)$ are localized close to, but inside the LCMS. The second maxima deep inside the confinement region are due to H- and He-like ions. They contribute about 30% to the total power loss $P(r) = 4\pi^2 R \int Q(r) r' \, dr'$. In view of the requirement of low radiation within the plasma core, nitrogen, radiating closer to the edge than neon should be favorable for relatively small devices such as W7-AS. Although for the same total power loss the central concentration is twice as high for nitrogen, the central dilution as expressed by the increase of Z_{eff} is the same as for neon. The titanium radiation is more smoothly distributed over the plasma cross section. The two maxima of the radiation profile arise from Na- and Mg-like ions and Li- and Be-like ions, respectively. They are clearly inside the confinement region. Therefore a reduction of the effective heating power $P_{heat} - P_{rad}$ associated with a significant degradation of energy confinement in the core has to be much more expected for titanium than for nitrogen. However, due to the small minor radius an influence of induced radiation on the central energy confinement seems to be possible even with nitrogen injection.

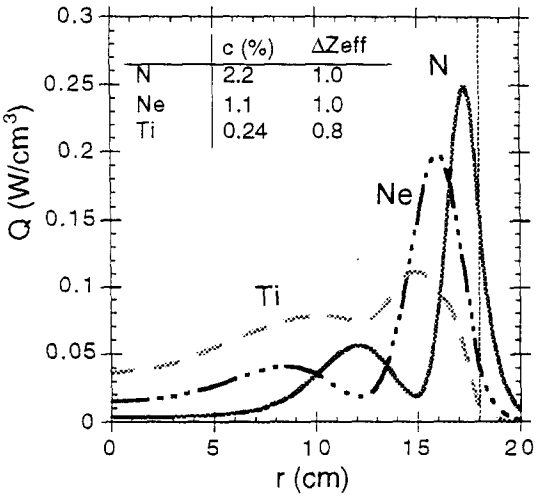

Fig. 2. Local emissivity $Q(r)$ calculated for the impurities nitrogen, neon and titanium (input parameters see text). The vertical line indicates the limiter position.

4. Experimental results and discussion

4.1. Nitrogen fuelling efficiency

Wall pumping of nitrogen [6] proved to be sufficiently high for feedback control. Decay times have been determined in a perturbation experiment with only small amount of nitrogen. After turning off the gas feed at the end of a phase of constant flow rate decay times of the order $\tau_1^* = 25 \pm 5$ ms for N IV have been measured (discharge conditions similar to those given in Section 3). The central chord soft-X radiation exhibits a bi-exponential decay. The fast decay time of about $\tau_2^* = 25 \pm 5$ ms is attributed to H- and He-like nitrogen. The slower decay time of about $\tau_3^* = 70$ ms is attributed to the transport of completely ionized particles from the plasma center, becoming radiative after recombination into H- and He-like ions.

The fuelling efficiency can be estimated by simple particle balance considerations. In steady state, the probability f_z that an injected impurity atom is confined in the plasma in the ionization state z is $f_z = N_z/(\Phi \tau_z^*)$, with the impurity flow rate Φ, the effective ion confinement time τ_z^*, and the number of ions N_z. The total fuelling efficiency is given by $f = \Sigma f_z$. We use $\tau_z^* = \tau_1^*$ for ions up to Be-like, τ_2^* for H- and He-like and τ_3^* for fully stripped ions. For the discharge parameters mentioned above an increase in soft-X radiation by an amount of 25 kW is observed when nitrogen is puffed at a moderate rate of $\Phi = 2.3 * 10^{20}$ s^{-1}. This increase can be simulated with the 1D code IONEQ by a total number of $1.4 * 10^{18}$ nitrogen ions. The contributions of the different charge states are 57%, for stripped ions, 36% for H- and He-like ions and 7% for ions up to Be-like. The central nitrogen concentration is 2.5%. From these data a total fuelling efficiency of only 15% is calculated.

Because of this low fuelling efficiency a large amount of nitrogen has to be introduced into the vessel, which due

to the high sticking probability leads to the shot-to-shot build-up of an intrinsic nitrogen reservoir. However, this reservoir settled at a stationary radiation level an order of magnitude lower than that resulting with injection. Short (10 min) helium glow discharge cleaning was not effective in reducing this internal reservoir, but it decreased after stellarator discharges without external nitrogen puff. Therefore, long-term contamination of the vessel with nitrogen was not observed.

4.2. Nitrogen puffing into limiter-dominated discharges

The spatial distribution of the total radiation is shown in Fig. 3 for a discharge which is simultaneously heated by 300 kW ECRH and 650 kW NBI power. For orientation, in the equatorial plane $z = 0$ the LCMS is located at $R = 0.178$ m (inboard) and at $R = 0.215$ m (outboard). In a reference discharge without nitrogen, intrinsic low Z impurities (boron, carbon) provide an already hollow radiation pattern, which appears asymmetrically enhanced at the outboard side. Nitrogen fuelling strongly increases edge radiation, in particular on the inboard side causing poloidally symmetric radiation in this case. The origin of these poloidal asymmetries in the low Z radiation pattern is not yet clear.

Time traces for the previous discharge with strong nitrogen puff ($\Phi = 5 * 10^{20}$ s^{-1}) and the unperturbed reference discharge are shown in Fig. 4. For both cases the deficiency between power loss (sum of radiated power and power flowing to the limiters) and heating power is less than 10% during the quasi steady phase ($|dW/dt| \ll P_{heat} = 950$ kW). The radiation increased from 20% to more than 60% of the input power causing a corresponding reduction of the limiter load. The electron temperature near the LCFS decreased from 70 to 25 eV. During the injection phase, both, the plasma stored energy and the central electron temperature degraded continuously with increasing radiation. The discharge recovered instantaneously on the nitrogen confinement time scale when the nitrogen puff was stopped.

The degradation can partly be explained by the global W7-AS confinement scaling [7] $\tau_E \sim P^{-0.55}$, i.e. $W \sim P^{0.45}$,

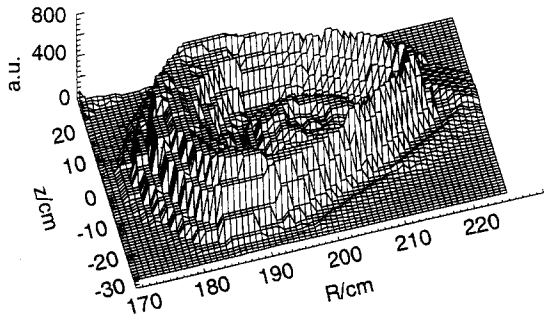

Fig. 3. Tomographically reconstructed radiation profiles from bolometry for a discharge with a strong nitrogen puff.

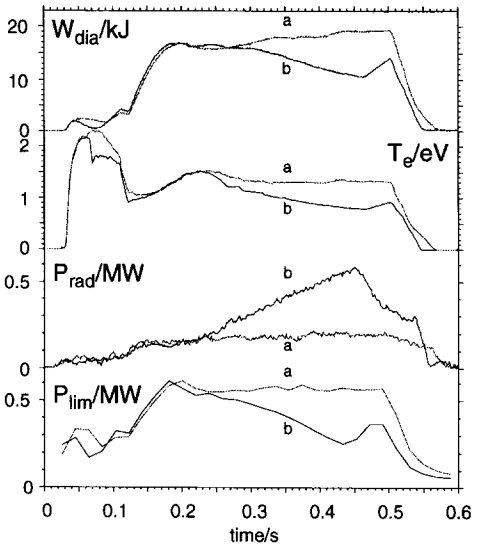

Fig. 4. Temporal traces of the diamagnetic energy, central electron temperature, radiated power and power loss to the limiters for a discharge of Fig. 3 with nitrogen puff from 0.25 to 0.45 s (b) and a reference discharge (a); $P_{heat} = 950$ kW, $\langle n_e \rangle = 7 * 10^{19}$ m^{-3}.

where $P = P_{heat} - P_{rad}$ with P_{rad} as the measured total radiated power. Better understanding has to be gained from an energy transport analysis accounting for the radial distribution of the radiative heat sink. If the radiation level is further increased the discharge becomes radiatively unstable. The maximum fraction of radiated power which could be maintained in quasi steady state increased with heating power from 33% at 200 kW to 60% at 1 MW.

4.3. Nitrogen injection into magnetic islands

The experiments have been performed with a nearly closed magnetic island, only intersected in the outermost region (ι about 0.570). The interaction of the plasma with the probe head is determined by the incident particle and power flux. With sufficiently high incident power an increase of the N IV emission line at 76.5 nm has always been observed indicating the release of nitrogen from the BN-ceramics. In contrast, emission lines of Ti (e.g., Ti XII) were scarcely found.

The injection caused a sudden increase of the plasma density and a decrease of the electron temperature in the edge plasma as observed earlier [8]. At line averaged densities higher than $1 * 10^{20}$ m^{-3} the probe induced plasma shrinking. For example in a discharge with $\langle n_e \rangle = 1.6 * 10^{20}$ m^{-3} the plasma density within the island measured by the probe itself decreased after a short sudden increase from $1.2 * 10^{20}$ m^{-3} before the injection to $2 * 10^{19}$ m^{-3} whereas the electron temperature dropped from about 60 eV to about 10 eV. This shrinking also observed by other Langmuir probes and the Li-beam was found to depend on the injected impurity amount indicated

by the intensity of the N IV-emission line. CCD-cameras viewing a lower limiter and the plasma edge tangentially at the inboard side with H α-filters showed plasma detachment from the limiter. These observations can be explained by a shift of the ionization zone towards the separatrix due to the strong decrease of the electron temperature in the island caused by the nitrogen injection. Results from a Langmuir probe array on the inboard side indicate that during the detachment the island configuration was not changed.

Considering the signals of the different bolometer channels it is generally found that radiation was mainly enhanced on the inboard side during the injection as observed with gas puffing in limiter-bounded discharges (see Section 4.2). At line averaged densities of $1.6*10^{20}$ m^{-3} strongly localized radiation zones at the inboard side (like MARFE's in tokamaks [9]) are induced by the impurity injection.

Fig. 5 shows the temporal evolution of the line integrated radiated power observed by the different bolometer channels in a contour plot for such a discharge. The probe

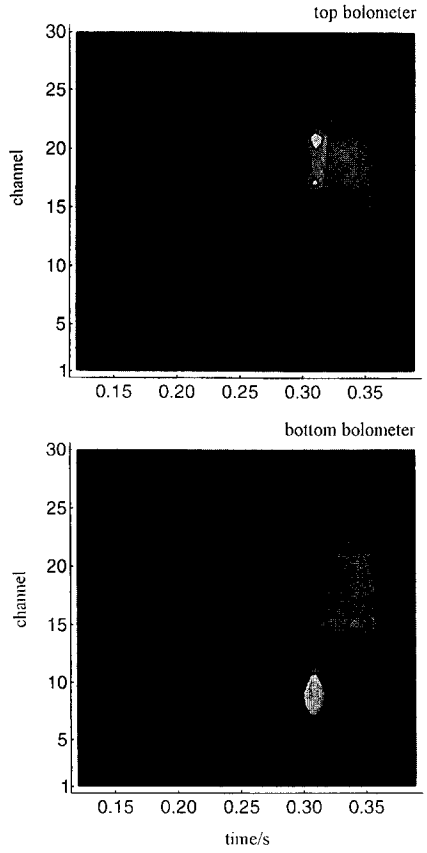

Fig. 5. Contourplot of the temporal evolution of the line integrated radiated power for the different channels of the top and bottom bolometer for a discharge with injection of nitrogen near the O-point region; $P_{heat} = 1.2$ MW, $\langle n_e \rangle = 1.6*10^{20}$ m^{-3}.

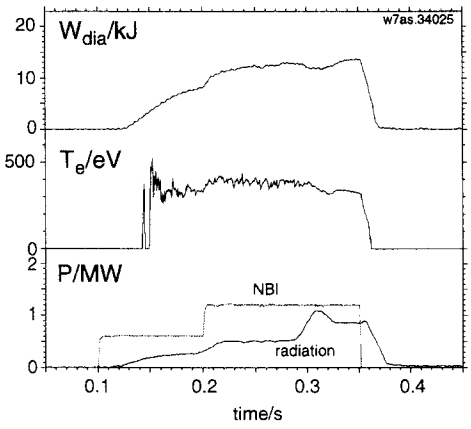

Fig. 6. Temporal traces of the diamagnetic energy, the central electron temperature, the heating and total radiated power for the discharge of Fig. 5.

electrode was at floating potential at approaching the region of the O-point at a time of 0.305 s to reduce the effects of the impurity injection compared to the biased case. The enhancement of the radiation during the impurity injection is clearly visible. Looking at the signals of the top bolometer it is obvious that the radiation pattern is influenced by the island topology at the plasma edge. The signals from the bottom bolometer clearly show that the region of strongly enhanced radiation is localized below the equatorial plane.

The total radiated power P_{rad} increased by a factor of about 2 due to the impurity injection (see Fig. 6). The radiating region near the lower limiter (Fig. 5) contributed significantly to this enhancement. This corresponds to the observed reduction of the peak power flux density on the lower limiter surface. The highest power load on the limiter as measured by thermography is restricted to a small region where the island boundary contacts the limiter surface. During the injection the power flux density decreased from 8 to 4 MW/m^2 in this contact region whereas the total power on the limiters P_{lim} decreased from 400 to 300 kW.

The stored plasma energy is transiently reduced by 10% during the injection which is in accordance with the fact that the power losses ($P_{rad} + P_{lim}$) exceeded transiently the heating power deposited in the plasma core. The central electron temperature dropped from 380 to 330 eV. The central Z_{eff} increased from 1.2 to 1.45 after the injection which can be explained by a central nitrogen concentration of 0.6%.

Nitrogen injection induced by a biased probe closer to the separatrix or exposing them near the X-point caused enhanced radiation in a belt above the equatorial plane which was in contact with the upper limiter. A simultaneous increase of N IV- and CIII-radiation lines were observed in these cases indicating forced erosion of carbon

from the upper limiter which then radiated in the vicinity as observed also by the CCD-cameras with CIII-filters. The camera which viewed the plasma tangentially revealed that the regions of enhanced radiation seems to be located near X-points. The increase of the central Z_{eff} and a corresponding decrease of the central electron temperature is much stronger in these cases. However, with the radiating region above the equatorial plane the peak power flux density to the lower limiter was reduced by 20% only which corresponds roughly to the degradation of the energy confinement in the core in that case.

5. Conclusions

Nitrogen proved to be appropriate for edge cooling studies in relatively small devices such as W7-AS because of its favorable recycling and radiation properties. Injection into the edge plasma caused enhanced radiation in particular on the inboard side of the torus. Cooling of the edge plasma and reduction of the limiter load was observed. The simultaneous degradation of the stored plasma energy is partly explained by the fact that the radiation shell occupies a significant fraction of the confinement volume and therefore reduces the effective heating power. This seems to limit the radiative stability and the maximum fraction of radiated power. A clear indication that nitrogen which was injected into a magnetic island caused radiation from island regions could not be found. However the different radiation pattern after injection near O-point and X-point regions is a first sign that the source position may be of importance for the impurity transport and radiation at the plasma edge.

References

[1] U. Samm et al., Plasma Phys. Control. Fusion 35 (1993) B167.
[2] A. Kallenbach et al., Nucl. Fusion 35 (1995) 1231.
[3] P. Grigull et al., these Proceedings, p. 935.
[4] A. Weller, JET-Report, JET-IR-(87)10.
[5] D. Naujoks et al., these Proceedings, p. 925.
[6] G.M. McCracken, B. Lipschitz, B. LaBombard et al., Proc. 22th Conf. on Controlled Fusion and Plasma Phys., Bournemouth, 1995, Part II, p. 313.
[7] U. Stroth et al., Nucl. Fusion, accepted for publication.
[8] D. Hildebrandt, Proc. 10th Int. Conf. on Stellarators, Madrid, 1995, p. 310.
[9] B. Lipschitz, B. LaBombard, E.S. Marmar et al., Nucl. Fusion 24 (1984) 977.